RESEARCH ARTICLE
SOLID EARTH: GEODYNAMICS

*Earth and Planetary Physics*
*10*: 13–21, 2026
doi: 10.26464/epp2026012

# Delaminated lower slab thermal regime before slab break-off in the Pamirs: Implications from 3D kinematic modeling

**Haris Faheem[1,2], YingFeng Ji[1,2*], Waqar Ahmed[1,2], Rui Qu[1,2], Ye Zhu[1,2], Fitriani Fitriani[1,2], Jun Yang[1,2], Shoichi Yoshioka[3,4], and Nobuaki Suenaga[3]**

[1]State Key Laboratory of Tibetan Plateau Earth System, Environment and Resources (TPESER), Institute of Tibetan Plateau Research, Chinese Academy of Sciences, Beijing 100101, China;

[2]University of Chinese Academy of Sciences, Beijing 100049, China;

[3]Research Center for Urban Safety and Security, Kobe University, Kobe 657-8501, Japan;

[4]Department of Planetology, Graduate School of Science, Kobe University, Kobe 657-8501, Japan

**Key Points:**

- Slab geometry with upper slab termination at shallow depths beneath the Pamirs is incorporated into kinematic modeling.
- The occurrence of intermediate-depth earthquakes aligns with cold slab regions near the slab tear-off below the southwestern Pamirs.
- The lateral asymmetry in slab temperature possibly explains the mechanism of lateral tearing and differential slab–mantle coupling.

**Citation:** Faheem, H., Ji, Y. F., Ahmed, W., Qu, R., Zhu, Y., Fitriani, F., Yang, J., Yoshioka, S., and Suenaga, N. (2026). Delaminated lower slab thermal regime before slab break-off in the Pamirs: Implications from 3D kinematic modeling. *Earth Planet. Phys.*, *10*(1), 13–21. http://doi.org/10.26464/epp2026012

**Abstract:** The intracontinental subduction of a >200-km-long section of the Tajik–Tarim lithosphere beneath the Pamir Mountains is proposed to explain nearly 30 km of shortening in the Tajik fold–thrust belt and the Pamir uplift. Seismic imaging revealed that the upper slab was scraped and that the lower slab had subducted to a depth of >150 km. These features constitute the tectonic complexity of the Pamirs, as well as the thermal subduction mechanism involved, which remains poorly understood. Hence, in this study, high-resolution three-dimensional (3D) kinematic modeling is applied to investigate the thermal structure and geometry of the subducting slab beneath the Pamirs. The modeled slab configuration reveals distinct along-strike variations, with a steeply dipping slab beneath the southern Pamirs, a more gently inclined slab beneath the northern Pamirs, and apparent upper slab termination at shallow depths beneath the Pamirs. The thermal field reveals a cold slab core after delamination, with temperatures ranging from 400 °C to 800 °C, enveloped by a hotter mantle reaching ~1400 °C. The occurrence of intermediate-depth earthquakes aligns primarily with colder slab regions, particularly near the slab tear-off below the southwestern Pamirs, indicating a strong correlation between slab temperature and seismicity. In contrast, the northern Pamirs exhibit reduced seismicity at depth, which is likely associated with thermal weakening and delamination. The central Pamirs show a significant thermal anomaly caused by a concave slab, where the coldest crust does not descend deeply, further suggesting crustal detachment or mechanical failure. The lateral asymmetry in slab temperature possibly explains the mechanism of lateral tearing and differential slab–mantle coupling.

**Keywords:** Pamirs; subduction; 3D kinematic modeling; slab geometry; intermediate-depth earthquake; crustal delamination; seismicity distribution

## 1. Introduction

The Pamir Mountains are located in the intracontinental subduction zone of the Tajik–Tarim lithosphere (TTL) in central Asia and are considered among the most seismically active regions at intermediate (70–300 km) depths (Figure 1; e.g., Pavlis and Das, 2000). The Pamir–Hindu Kush Mountains extend northwest from Tibet and represent one of the most integral components of the Earth's extensive active continental collision (Kufner et al., 2016). Since the Paleozoic era, the western Himalayan syntaxis orogen has included Gondwana-derived microcontinents and subduction–accretion–arc complexes (Schwab et al., 2004), which have been affected by the collision between the Indian and Eurasian Plates since the early Cenozoic (Yin A and Harrison, 2000; Morley, 2002). The complex tectonic history of this area has resulted in exceptionally high stress levels, rapid rates of uplift and erosion, and increased occurrence of metamorphic and magmatic events within the orogenic belt (Zhang ZM et al., 2007; Xu ZQ et al., 2011; Kufner et al., 2016; Mir et al., 2017). Therefore, the Pamir region is among the most seismically active zones globally, with seismicity concentrated at intermediate to deep depths (Figure 1). However,

First author: H. Faheem, haris@itpcas.ac.cn
Correspondence to: Y. F. Ji, yingfengji@itpcas.ac.cn
Received 27 JUN 2025; Accepted 30 SEP 2025.
First Published online 10 NOV 2025.

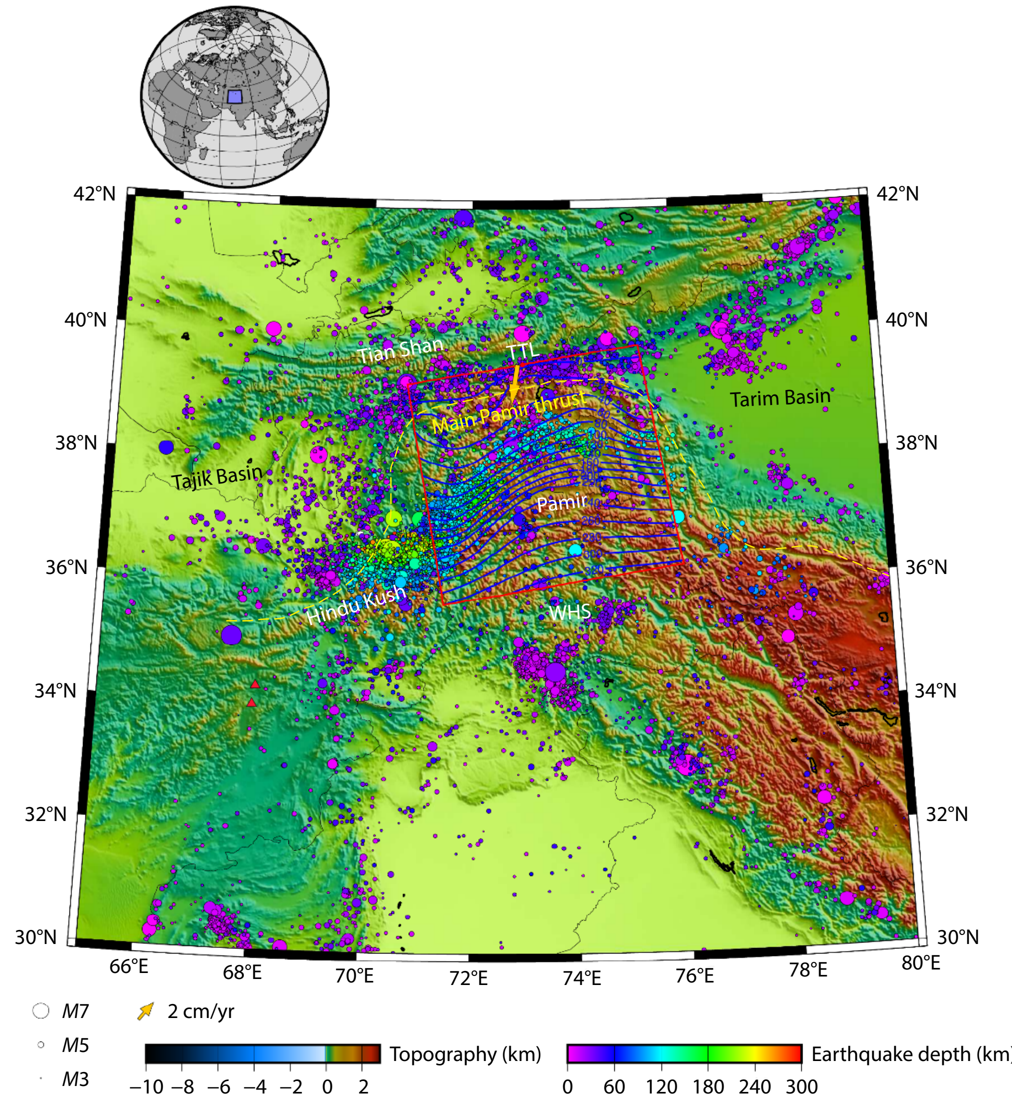


**Figure 1**. Tectonic framework and topography of the Pamirs. Background colors indicate the surface topography (ETOPO; Smith and Sandwell, 1997). The red box indicates the study area. The blue curved lines denote the isodepth contours of the slab upper surface at intervals of 20 km and are extrapolated using Slab2 data (Hayes et al., 2018). The yellow arrow indicates the motion of the incoming plate toward the overriding plate (MORVEL; DeMets and Dixon, 1999; DeMets et al., 2010). The solid colored circles represent the observations of magnitude >3 earthquakes from 2000 to 2024 (IRIS: Trabant et al., 2012). The dashed yellow line indicates the main Pamir thrust. TTL, Tajik–Tarim lithosphere; WHS, western Himalayan syntaxis.

the deep structure and tectonic evolution in neighboring areas are still poorly understood (Negredo et al., 2007; Cowgill, 2010; Sippl et al., 2013a).

The Pamir–Hindu Kush region, Kohistan arc, and Karakorum terrane are the main components of the western Himalayan syntaxis. This tectonic framework is shaped by the India–Eurasia collision orogen (Yin A and Harrison, 2000; Jadoon et al., 2021). Accretion began in the early Cenozoic and is ongoing at present, with a convergence rate of approximately 34 mm/yr adjacent to the western Himalayan syntaxis (Molnar and Stock, 2009; DeMets et al., 2010). The Pamir crust has a maximum thickness of ~90 km and an elevation of approximately 4 km above sea level (Schmidt et al., 2011; Schneider et al., 2019; Xu Q et al., 2021). To the east of the Pamirs is the Tarim Basin, to the north is the Tian Shan, and to the west is the Tajik Basin. The Pamirs, with their curvature to the north, formed during the push of the TTL from the north, most likely beginning at approximately 25 Ma (e.g., Schwab et al., 2004; Chapman et al., 2017). There is also evidence that the Pamirs have been displaced by at least 300 km relative to Tibet on the basis of the observed offset and curvature of the accretionary boundary and terranes near the western Himalayan syntaxis (e.g., Burtman and Molnar, 1993; Molnar and Stock, 2009; DeMets et al., 2010). To accommodate the large component of northward convergence, many thrusts and strike-slip faults have developed across the Pamirs (Sobel et al., 2011, 2013; Robinson et al., 2015), including the main Pamir thrust and the South Tian Shan thrust in the northern part of the study area (Coutand et al., 2002).

This study aims to utilize three-dimensional (3D) high-resolution kinematic thermal models to examine the thermal structure and dynamics of the subducting continental lithosphere beneath the Pamir orogen. The model incorporates the slab geometry (including slab detachment and break-off), temperature distribution, and seismicity patterns to explore the spatial variability in slab thermal regimes. Specific emphasis is placed on evaluating the thermal weakening, stagnation, and detachment of the cold crust in the northern Pamirs. This study also aims to explore the temperature contrast of the slab between the eastern and western flanks to better understand possible lateral slab tearing or the exchange of complexities between the slab and the ambient mantle. These tests are discussed within the framework of continental collision zones, and the findings are compared with those of previous models from studies on mature subduction systems (e.g., Ji YF et al., 2016, 2017, 2021; Zhu WL et al., 2022; Qu R et al., 2023; Zhu Y et al., 2023).

## 2. Methods and Models

To study the complex subduction dynamics and geometry of the Pamirs, which formed the collision zone, we constructed a 3D thermomechanical model by using the Stage3D code (Tackley and Xie S, 2003). This model incorporates a kinematic slab guide based on geological and seismological evidence, including slab delamination and break-off. The model dimensions were 400 km in length, 400 km in width, and 400 km in depth (Figure 2), with 72 × 72 × 72 grid points. The initial shape of the slab geometry was set via the Slab2 global subduction zone model, and slab dips were adjusted according to seismic activity in different regions (Hayes et al., 2018). A schematic diagram of the model setup and boundary conditions is shown in Figure S1 in the Supplementary Materials. The subduction velocities were derived from the MORVEL plate motion model (DeMets et al., 2010). The initial thermal states of the slab and mantle were determined using a plate cooling model (Grose and Afonso, 2013) for both the overriding plate and the incoming plate (>100 Myr). The temperature calculations in the model simulate the thermal evolution of the overriding and subducting plates as they age. The modeling was performed over a 50 Myr timescale, during which the system reached a steady-state thermal regime, and the results presented reflect the thermal equilibrium achieved at the end of the calculation period.

The mechanical boundary conditions included the top as a rigid surface with a fixed temperature (0 °C), whereas the four vertical boundaries (front, back, left, and right) and the bottom were set as permeable and adiabatic, respectively. The model uses composite rheology for wet olivine in the upper mantle (Hirth and Kohlstedt, 2004), which includes both diffusion and dislocation creep. The thickness of the slab is dependent on plate age (Yoshii, 1975). Model validation involved the integration of various geophysical datasets. The distributions of earthquakes are from the IRIS datasets (Figures 1 and 3a; Trabant et al., 2012). The accuracy resolution was revealed by comparing steady-state temperature values from the 72 × 72 × 72 and 84 × 84 × 84 mesh configurations, and the resulting difference was less than 2%. More details about the parameters are included in the Supplemental Materials.

## 3. Results

### 3.1 3D Slab Geometry and Subduction Velocity

The 3D arrangement of the lithospheric slab beneath the Pamirs is depicted in Figure 2, which provides a comprehensive representation of its shape and depth distribution derived from Slab2. This

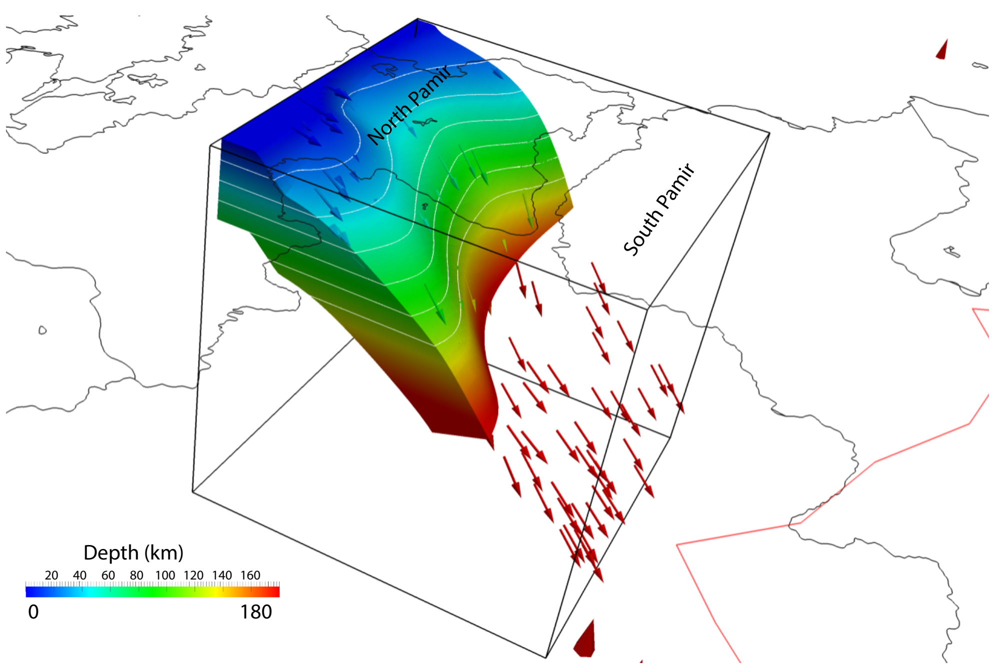


**Figure 2**. Three-dimensional geometry and subduction kinematics of the Pamir slab. The color of the slab indicates the depth (km). The colored arrows indicate the slab motion and induced mantle flows. The white lines indicate the isodepth contours of the Pamir slab from 20 to 120 km at an interval of 20 km.

figure also outlines the slab motion as it descends into the mantle. Large differences are apparent in the slab structure dip angles from region to region. The depth contours begin at 20 km near the convergence strike and extend to approximately 120 km, approaching the slab break-off depth (150–180 km). The superimposed red vectors represent the subduction velocity field, which ranges between 3.6 and 3.7 mm/yr. This velocity range suggests a relatively steady and uniform subduction process across the arcuate segment. It is interesting that the slab appears to terminate or become discontinuous beneath the central Pamir region. This limited variation may reflect thermal weakening, mechanical decoupling, or a transition from a cold, brittle slab to a warmer, more ductile regime that inhibits further penetration. Such slab stagnation is consistent with the observed seismic gaps at greater depths and may suggest that the slab is either thermally eroded or has encountered resistance at depth, possibly because of changes in mantle rheology or buoyant crustal components within the subducting lithosphere, which facilitates slab break-off.

The overall geometry supports the hypothesis of a “scraped” or “detached” slab system beneath the Pamirs, where the upper crust of the slab was scraped and incorporated into the overriding Pamir crust and subducted at a shallow depth according to seismic imaging (e.g., Schneider et al., 2013). The lower portion of the slab may have undergone delamination or break-off at depths of 150–180 km (e.g., Kufner et al., 2016). This behavior aligns with geophysical evidence for complex slab dynamics in continental collision zones, where the cold lower crust often fails to subduct fully because of its buoyancy and thermal structure.

### 3.2 Thermal Structure and Earthquake Distribution

Figure 3a shows the modeled thermal structure of the subducting slab beneath the Pamir orogen at the plate interface, which is superimposed on the earthquake hypocenters. The size and color of the spheres correspond to the earthquake magnitude. The thermal model reveals a distinctly cold slab core, with temperatures ranging from approximately 400 °C to 800 °C. This cold core is surrounded by the asthenospheric mantle, which reaches significantly higher temperatures, ~1400 °C, resulting in a pronounced thermal contrast. Such a thermal gradient is characteristic of active subduction zones and plays a critical role in governing slab strength, seismicity, and dehydration processes.

In the central Pamir region, the cold crustal portion of the slab is notably absent at greater depths. This spatial discontinuity in the thermal field suggests that the lower portion of the slab, particularly the ultramafic lower crust or underlying lithospheric mantle, may have undergone thermal erosion, mechanical delamination, or detachment. The absence of a cold, high-density slab at these depths implies that the lithosphere has either stagnated or been assimilated into the surrounding mantle, potentially owing to the buoyant nature of the continental crust or enhanced incorporation into the Pamirs in this collisional setting.

Seismicity patterns provide additional support for this interpretation. In the southern Pamirs, where the slab remains cold and mechanically cohesive, earthquake hypocenters are very close together along the slab contact (Figure 3a). This configuration favors brittle failure and intermediate-depth seismicity. These events include earthquakes with magnitudes >4, which means that the strength and internal stress of the slab still cause major seismic rupture. On the other hand, the distribution of earthquakes in the northern Pamirs has become much less frequent and shallower, with clear decreases in both frequency and magnitude. This seismic quiescence correlates spatially with the thermally weak-

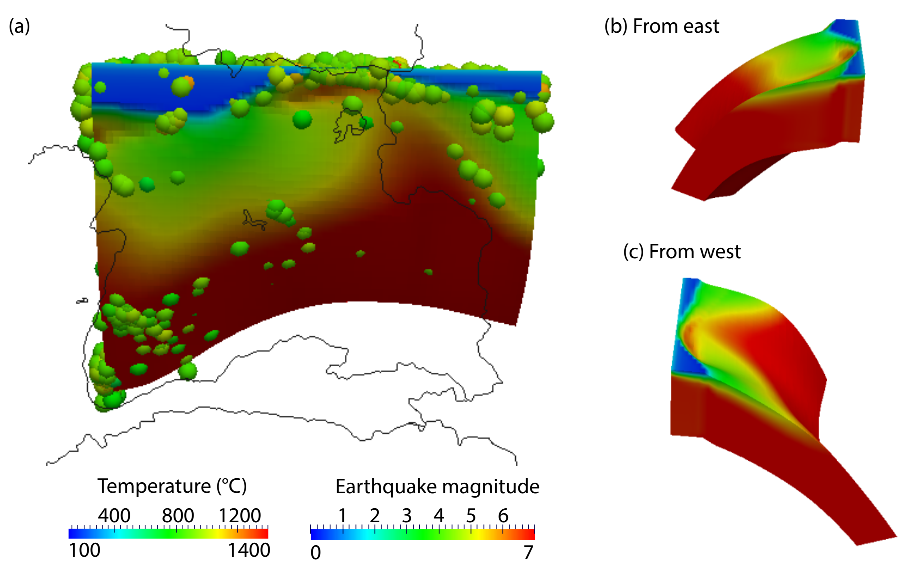


**Figure 3**. (a) Horizontal view of the steady-state thermal structure (°C) at the plate interface calculated in this study. The thermal field is overlain by earthquake hypocenters of varying magnitudes. Compared with the surrounding mantle (~1400 °C), the slab core remains cold (400–800 °C). Seismicity is concentrated along the slab interface in the southern Pamirs but becomes sparse in the northern Pamirs, supporting possible slab detachment or thermal erosion. (b–c) Vertical cross sections showing the modeled thermal structure of the subducting slab. Eastward and westward views of the slab temperature distribution reveal thermal asymmetry. The eastern flank is colder than the western flank, implying lateral tearing or complex slab–mantle interactions.

ened or absent slab segment and implies a transition to a more ductile or fragmented regime incapable of generating high-magnitude seismic events. The lack of seismicity deeper than 180 km may be attributed to slab break-off, progressive thermal weakening, or complete detachment of the subducting lithosphere.

Overall, the observed thermal structure and seismicity distribution point toward a heterogeneous slab architecture beneath the Pamirs, where ongoing subduction is active and seismically energetic in the southern segment but disrupted or absent in the central and northern segments. These patterns are consistent with a tectonic scenario involving slab fragmentation, lower crustal buoyancy, and complex slab–mantle interactions, all of which contributed to the unique geodynamic evolution of the Pamir collision zone.

### 3.3 Asymmetric Thermal Anomalies from Different Perspectives

Oblique views of the thermal distribution of the subducting slab from the eastern and western perspectives are shown in Figures 3b and 3c, respectively. These visualizations provide crucial insights into the 3D nature of the thermal regime of the slab beneath the Pamir orogen.

From the eastern view (Figure 3b), the slab appears sharply delineated by colder temperatures, with a well-preserved thermal contrast between the slab and surrounding mantle. The cold slab core is more coherent and continuous on this flank, suggesting that the thermal and mechanical integrity of the slab is maintained at greater depths. These observations may reflect stronger coupling with the overriding lithosphere or less disruption of the subduction process on the eastern side.

In contrast, the middle portion of the convergence margin reveals markedly different thermal signatures (e.g., Figure 3c). Here, the slab appears to have higher temperatures, with the cold core becoming diffuse or absent. The increased thermal gradient and reduced upper crust imply greater heating from the surrounding mantle and possibly a more advanced stage of slab weakening or detachment. These higher temperatures and thermal states may result from enhanced mantle upwelling, slab rollback, or lateral asthenospheric flow, all of which could promote thermal erosion of the slab margins.

The observed east–west thermal asymmetry points toward lateral variations in slab dynamics, which could be the result of oblique slab subduction or variable crustal properties along the orogenic front. Such asymmetry is commonly associated with complex slab–mantle interaction zones, where the geometry and dynamics of the subducting plate are influenced by inherited lithospheric heterogeneities or changes in slab buoyancy and strength.

The slab asymmetry observed in the vertical slices (Figures 3b–3c) suggests a laterally variable subduction regime. The distributions of earthquakes in cooler thermal zones and margins of the slab are particularly concentrated in the northwest, suggesting that the thermal regime plays an important role in defining the earthquake distribution. Conversely, in south-central Pamir, subducted plate seismicity is less prominent, which may reflect slab erosion associated with deep crustal failure or thermal effects.

## 4. Discussion

### 4.1 Slab Geometry and Seismic Implications

A complex subduction geometry with different slab dip angles and termination depths is evident in the 3D slab beneath the Pamirs. On the basis of previous seismic and tomographic imaging, the slab flattens after dipping steeply beneath the southern Pamirs (Sippl et al., 2013b; Kufner et al., 2016). The slab may not appreciably return or break off, as suggested by stable but weak rollback. Nevertheless, the observed flatlike termination of the slab at shallow upper mantle depths beneath the central Pamirs implies either piling up or thermal weakening at depth (Stearns et al., 2015).

Furthermore, the slab geometry fits with the pattern of observed seismicity. Intermediate-depth earthquakes are tightly clustered near the axis of the cold slab, particularly under the southern Pamirs (Pavlis and Das, 2000). In contrast, slab retreat and potential slab tear or delamination are associated with decreased seismicity to the north. These findings confirm the proposal that the slab morphology and thermal regime play fundamental roles in the combination of the depth distribution and the number of earthquakes (Zhao DP, 2001).

The calculated saturation temperatures are highly relevant for determining the behavior of the interaction between the slab and mantle forearc. A hot mantle wedge (with temperatures >1200 °C) reminiscent of an annulus around a cold (400 °C–800 °C) central portion of the slab has been used to describe the interiors of subducted slabs in mature subduction zones (Syracuse et al., 2010). Lateral asymmetries are also ubiquitous. The oblique perspectives (Figures 3b and 3c) indicate that the easterly flank of the slab is considerably cooler than the westerly flank. The gap probability may instead reflect slab fragmentation, the subduction angle, or lateral variations in the slab–mantle interaction and the thermal distribution itself in the subarc asthenosphere (Zhong SJ et al., 2000; Faccenda and Capitanio, 2013). This heterogeneity may be due to different convergence velocities along the strike or inherited lithospheric weakness.

Thermal fluctuations are associated with changes in seismicity. The hotter middle part of the margin, with higher thermal gradients, is seismically less active than the cooler eastern and northern parts, which corresponds to more active earthquakes.

### 4.2 Thermal State and Lateral Variability

The thermal modeling results reveal a distinct variation in the thermal regime of the slab along both the dip direction and the strike beneath the Pamirs. Cross-sectional views (Figure 3a) reveal that the subducting slab contains a cold core, with temperatures ranging between approximately 400 °C and 800 °C, surrounded by ambient mantle temperatures exceeding 1300 °C. This cold thermal signature is consistent with subduction-related cooling of the lithosphere and is in agreement with similar findings from global subduction zones (Peacock, 2004; Peacock et al., 2005).

It is important to note that the cold crust of the slab appears discontinuous in the central Pamirs and fails to extend to greater depths than adjacent regions do. These observations may indicate thermal weakening of the lower crust at mid-mantle depths. Such processes have been proposed in the context of continental collision zones, where high heat flow and buoyant crustal materials lead to detachment of the dense lower crust from the overlying lithosphere (Li C et al., 2008). The localized weakening of the thermal structure supports a potential scenario of crustal delamination beneath the central Pamirs, which may play a role in moderating subduction dynamics and influencing slab continuity.

Plan-view slices (Figures 3b–3c) highlight an asymmetric thermal distribution: the eastern and western segments of the slab remain relatively cooler, whereas the middle portion of the margin has higher temperatures. This asymmetry may arise via lateral slab ripening, differential mantle movement, or varying degrees of hydration of the subducting crust, as reported in other tectonic systems (e.g., Zhu Y et al., 2023). This dynamic interaction between the slab and the mantle may involve lateral tearing or off-balance mantle flow.

The relationship between slab temperature and earthquake distribution also highlights the importance of temperature-controlled processes, such as dehydration embrittlement, in intermediate-depth seismicity (Hacker et al., 2003). These findings suggest that intense seismicity is associated with the cold slab interface. Heat conditions strongly influence the mechanical behavior and characteristics of earthquakes in the context of continental subduction.

Slab break-off initiates when slab pull forces, driven by the density contrast between the descending slab and surrounding mantle, surpass the viscous resistance of the mantle, resulting in localized necking and eventual rupture (Duretz et al., 2012). The detachment process can be initiated after a prolonged period (8–30 Myr) of slab weakening caused by thermal diffusion, after which a rapid detachment process occurs over a few million years (Gerya et al., 2004). The timing and depth of break-off are strongly influenced by the slab rheology. Stronger slabs (e.g., yield strength of ~500 MPa) detach deeply and slowly, whereas weaker slabs (~300 MPa) break off more rapidly and at shallower depths (Andrews and Billen, 2009).

### 4.3 Comparison with the Pressure–Temperature Conditions of Exhumed Rocks in the Pamirs

The pressure–temperature (P–T) conditions of rock samples from the Pamir lithosphere from previous studies and the estimated P–T conditions of the upper surface of the subducted TTL (dashed blue line) according to the model results are presented in Figure 4. Notably, the results indicate that the slab surface is, on average, 100 °C cooler than the surrounding mantle wedge at the continental Moho depth. This difference decreases to approximately 50 °C at the Pamir Moho depth. When the depth exceeds 100 km, the difference in temperature between the slab and overriding mantle decreases to less than 30 °C. This result captures the along-strike variation in the calculated slab thermal regime and compares well with the P–T conditions (hotter) of the samples from the overriding lithosphere according to previous geological

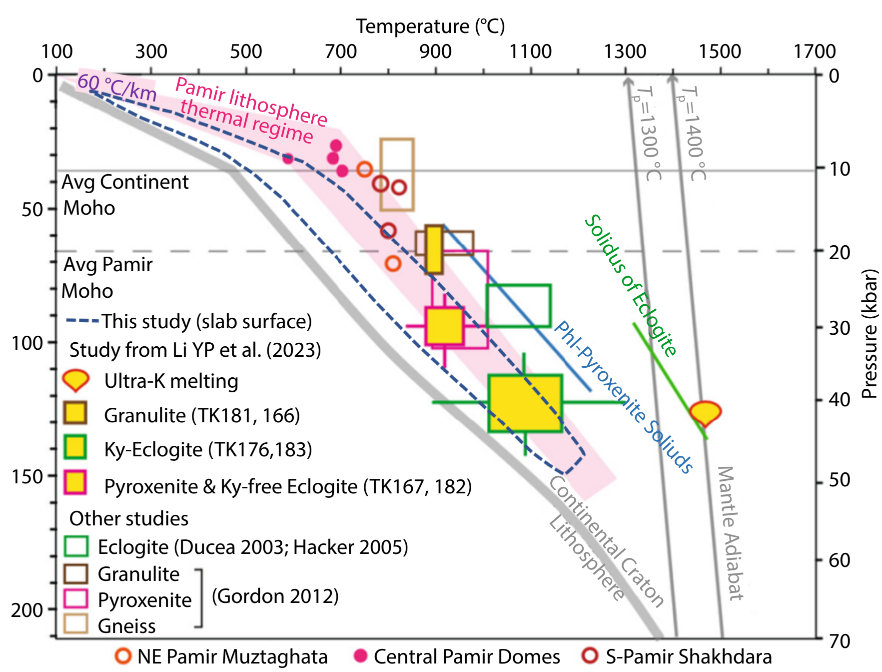


**Figure 4**. Comparison with the P–T conditions of exhumed rocks in the Pamirs (modified from Li YP et al., 2023), including xenoliths based on depth-affinity relations (Li YP et al., 2023), the continental craton (McKenzie et al., 2005), the Muztaghata dome (Robinson et al., 2007; Li YP et al., 2020a, b), and the central–southern Pamir domes (Schmidt et al., 2011; Hacker et al., 2017). The empty colored boxes indicate other previous studies, with the first author and publication year annotated (Ducea et al., 2003; Hacker et al., 2005; Gordon et al., 2012). The pink area indicates a geothermal gradient of 60 °C/km (Stübner et al., 2013). The dashed blue line indicates the P–T trajectory of the upper surface of the subducted slab obtained from this study. $T_{\rm p}$ is temperature at constant pressure.

studies in the Pamirs (granite, eclogite, pyroxene, and gneiss).

The P–T variation in the subducted lithosphere indicates that below a depth of 150 km, the upper surface temperatures of the slab are almost the same as those of the ambient mantle, which implies that the slab core temperature has greatly increased at this depth. This is conducive to lower crustal detachment, slab melting or break-off, and the occurrence of deep earthquakes (150–180 km), which feature the Pamir tectonic system.

Although this study, which is based on a 3D kinematic model, provides first-order insights into the thermal structure of the Pamir slab, the lack of geophysical constraints limits our ability to fully investigate the uncertainties. Thus, further analyses to evaluate model robustness on the basis of geophysical observations are necessary.

## 5. Conclusions

On the basis of the 3D kinematic modeling, we reached the following conclusions:

(1) The structure of the subducting plate beneath the Pamirs is thermally and mechanically segmented, with significant variations in dip angle and seismic activity across the region. The upper slab appears to terminate at shallow depths beneath the Pamirs, indicating a dynamic interaction between the slab and the mantle that involves lateral tearing or off-balance mantle flow. This provides a clear case study for how continental slabs may disaggregate through tearing, a process that is likely critical to the evolution of other complex collisional orogens, such as the Himalayas or the Alps.

(2) The nonuniform temperature distribution, with colder temperatures in the east and warmer temperatures in the west, highlights the complexity of slab–mantle interactions. The correlation of the thermal structure with seismicity supports the idea that temperature-controlled processes play crucial roles in generating earthquakes and maintaining slab stability. Our 3D model quantitatively links thermal anomalies to seismic clusters, offering a new framework for interpreting seismicity in subduction zones where direct thermal constraints are absent.

(3) This study highlights the importance of integrating thermal modeling with seismological data to gain deeper insights into the lithospheric dynamics beneath continental collision zones, such as the Pamirs. More broadly, this study demonstrates that the integration of high-resolution 3D kinematic modeling with seismological data is a powerful tool for elucidating lithospheric dynamics. We underscore that this approach is not limited to the Pamirs but is essential for gaining deeper insights into continental collision zones globally. We recommend that future research focus on applying similar multidisciplinary workflows to other complex subduction systems to better constrain thermomechanical controls on slab deformation and earthquake genesis. This work contributes to our understanding of subduction processes and slab behavior at greater depths.

## Acknowledgments

This study benefited from the financial support of the Chinese Academy of Sciences Pioneer Hundred Talents Program and the Second Tibetan Plateau Scientific Expedition and Research Program (Grant No. 2019QZKK0708). This work was partly supported by a MEXT (Ministry of Education, Culture, Sports, Science and Technology) KAKENHI (Grants-in-Aid for Scientific Research) grant (Grant No. 21H05203) and Kobe University Strategic International Collaborative Research Grant (Type B Fostering Joint Research). We thank P. Tackley for sharing the original Stage3D code that was used in our study. Figures were created via Generic Mapping Tools and ParaView software developed by Kitware, Inc. We also gained knowledge through the support of computing facilities provided by the Institute of Tibetan Plateau Research, including the Sugon supercomputing platform and workstations.

## Author Contributions

Y.J. conceived of the original idea, designed the 3D thermomechanical code, and performed the numerical experiments. H.F. interpreted the results and wrote the manuscript. Y.J., W.A., R.Q., Y.Z., F.F., J.Y., S.Y., and N.S. provided comments to improve the manuscript.

## Competing Interests

All the authors declare that they have no competing interests.

## Data Availability Statements

In this study, we used plate data from Slab2 (Hayes et al., 2018, https://doi.org/10.1126/science.aat4723) and the MORVEL plate motion dataset (DeMets et al., 2010, https://doi.org/10.1111/j.1365-246X.2009.04491.x).

## References

Andrews, E. R., and Billen, M. I. (2009). Rheologic controls on the dynamics of slab detachment. *Tectonophysics*, *464*(1–4), 60–69. https://doi.org/10.1016/j.tecto.2007.09.004

Burtman, V. S., and Molnar, P. (1993). *Geological and Geophysical Evidence for Deep Subduction of Continental Crust Beneath the Pamir. Volume 281*. Boulder, CO: Geological Society of America. https://doi.org/10.1130/SPE281

Chapman, J. B., Carrapa, B., Ballato, P., DeCelles, P. G., Worthington, J., Oimahmadov, I., Gadoev, M., and Ketcham, R. (2017). Intracontinental subduction beneath the Pamir Mountains: Constraints from thermokinematic modeling of shortening in the Tajik fold-and-thrust belt. *GSA Bull.*, *129*(11–12), 1450–1471. https://doi.org/10.1130/b31730.1

Coutand, I., Strecker, M. R., Arrowsmith, J. R., Hilley, G., Thiede, R. C., Korjenkov, A., and Omuraliev, M. (2002). Late Cenozoic tectonic development of the intramontane Alai Valley, (Pamir-Tian Shan region, central Asia): An example of intracontinental deformation due to the Indo-Eurasia collision. *Tectonics*, *21*(6), 1053. https://doi.org/10.1029/2002TC001358

Cowgill, E. (2010). Cenozoic right-slip faulting along the eastern margin of the Pamir salient, northwestern China. *GSA Bull.*, *122*(1–2), 145–161. https://doi.org/10.1130/B26520.1

DeMets, C., and Dixon, T. H. (1999). New kinematic models for Pacific-North America motion from 3 Ma to present, I: Evidence for steady motion and biases in the NUVEL-1A model. *Geophys. Res. Lett.*, *26*(13), 1921–1924. https://doi.org/10.1029/1999GL900405

DeMets, C., Gordon, R. G., and Argus, D. F. (2010). Geologically current plate motions. *Geophys. J. Int.*, *181*(1), 1–80. https://doi.org/10.1111/j.1365-246X.2009.04491.x

Ducea, M. N., Lutkov, V., Minaev, V. T., Hacker, B., Ratschbacher, L., Luffi, P., Schwab, M., Gehrels, G. E., McWilliams, M., ... Metcalf, J. (2003). Building the Pamirs: The view from the underside. *Geology*, *31*(10), 849–852. https://doi.org/10.1130/G19707.1

Duretz, T., Schmalholz, S. M., and Gerya, T. V. (2012). Dynamics of slab detachment. *Geochem. Geophys. Geosyst.*, *13*(3), Q03020. https://doi.org/10.1029/2011GC004024

Faccenda, M., and Capitanio, F. A. (2013). Seismic anisotropy around subduction zones: Insights from three-dimensional modeling of upper mantle deformation and SKS splitting calculations. *Geochem. Geophys. Geosyst.*, *14*(1), 243–262. https://doi.org/10.1002/ggge.20055

Gerya, T. V., Yuen, D. A., and Maresch, W. V. (2004). Thermomechanical modelling of slab detachment. *Earth Planet. Sci. Lett.*, *226*(1–2), 101–116. https://doi.org/10.1016/j.epsl.2004.07.022

Gordon, S. M., Luffi, P., Hacker, B., Valley, J., Spicuzza, M., Kozdon, R., Kelemen, P., Ratshbacher, L., and Minaev, V. (2012). The thermal structure of continental crust in active orogens: Insight from Miocene eclogite and granulite xenoliths of the Pamir Mountains. *J. Metamorph. Geol.*, *30*(4), 413–434. https://doi.org/10.1111/j.1525-1314.2012.00973.x

Grose, C. J., and Afonso, J. C. (2013). Comprehensive plate models for the thermal evolution of oceanic lithosphere. *Geochem. Geophys. Geosyst.*, *14*(9), 3751–3778. https://doi.org/10.1002/ggge.20232

Hacker, B. R., Peacock, S. M., Abers, G. A., and Holloway, S. D. (2003). Subduction factory 2. Are intermediate-depth earthquakes in subducting slabs linked to metamorphic dehydration reactions?. *J. Geophys. Res.: Solid Earth*, *108*(B1), 2030. https://doi.org/10.1029/2001JB001129

Hacker, B. R., Luffi, P., Lutkov, V., Minaev, V., Ratschbacher, L., Plank, T., Ducea, M., Patiño-Douce, A., McWilliams, M., and Metcalf, J. (2005). Near-ultrahigh pressure processing of continental crust: Miocene crustal xenoliths from the Pamir. *J. Petrol.*, *46*(8), 1661–1687. https://doi.org/10.1093/petrology/egi030

Hacker, B. R., Ratschbacher, L., Rutte, D., Stearns, M. A., Malz, N., Stübner, K., Kylander-Clark, A. R. C., Pfänder, J. A., and Everson, A. (2017). Building the Pamir-Tibet Plateau—Crustal stacking, extensional collapse, and lateral extrusion in the Pamir: 3. Thermobarometry and petrochronology of deep Asian crust. *Tectonics*, *36*(9), 1743–1766. https://doi.org/10.1002/2017TC004488

Hayes, G. P., Moore, G. L., Portner, D. E., Hearne, M., Flamme, H., Furtney, M., and Smoczyk, G. M. (2018). Slab2, a comprehensive subduction zone geometry model. *Science*, *362*(6410), 58–61. https://doi.org/10.1126/science.aat4723

Hirth, G., and Kohlstedt, D. (2004). Rheology of the upper mantle and the mantle wedge: A view from the experimentalists. In J. Eiler (Ed.), *Inside the Subduction Factory, Volume 138* (pp. 83–105). Washington, DC: American Geophysical Union. https://doi.org/10.1029/138GM06

Jadoon, I. A. K., Ding, L., Jadoon, S. R. K., Bhatti, Z. I., Shah, S. T. H., and Qasim, M. (2021). Lithospheric deformation and active tectonics of the NW Himalayas, Hindukush, and Tibet. *Lithosphere*, *2021*(1), 7866954. https://doi.org/10.2113/2021/7866954

Ji, Y. F., Yoshioka, S., and Matsumoto, T. (2016). Three-dimensional numerical modeling of temperature and mantle flow fields associated with subduction of the Philippine Sea plate, southwest Japan. *J. Geophys. Res.: Solid Earth*, *121*(6), 4458–4482. https://doi.org/10.1002/2016JB012912

Ji, Y. F., Yoshioka, S., and Banay, Y. A. (2017). Thermal state, slab metamorphism, and interface seismicity in the Cascadia subduction zone based on 3-D modeling. *Geophys. Res. Lett.*, *44*(18), 9242–9252. https://doi.org/10.1002/2017GL074826

Ji, Y. F., Yan, R. Y., Zeng, D., Xie, C. D., Zhu, W. L., Qu, R., and Yoshioka, S. (2021). Slab dehydration in Sumatra: Implications for fast and slow earthquakes and arc magmatism. *Geophys. Res. Lett.*, *48*(3), e2020GL090576. https://doi.org/10.1029/2020GL090576

Kufner, S. K., Schurr, B., Sippl, C., Yuan, X. H., Ratschbacher, L., Akbar, A. S. M., Ischuk, A., Murodkulov, S., Schneider, F., ... Tilmann, F. (2016). Deep India meets deep Asia: Lithospheric indentation, delamination and break-off under Pamir and Hindu Kush (Central Asia). *Earth Planet. Sci. Lett.*, *435*, 171–184. https://doi.org/10.1016/j.epsl.2015.11.046

Li, C., Van der Hilst, R. D., Meltzer, A. S., and Engdahl, E. R. (2008). Subduction of the Indian lithosphere beneath the Tibetan Plateau and Burma. *Earth Planet. Sci. Lett.*, *274*(1–2), 157–168. https://doi.org/10.1016/j.epsl.2008.07.016

Li, Y. P., Robinson, A. C., Gadoev, M., and Oimuhammadzoda, I. (2020a). Was the Pamir salient built along a Late Paleozoic embayment on the southern Asian margin?. *Earth Planet. Sci. Lett.*, *550*, 116554. https://doi.org/10.1016/j.epsl.2020.116554

Li, Y. P., Robinson, A. C., Lapen, T. J., Righter, M., and Stevens, M. K. (2020b). Muztaghata dome Miocene eclogite facies metamorphism: A record of lower crustal evolution of the NE Pamir. *Tectonics*, *39*(7), e2019TC005917. https://doi.org/10.1029/2019TC005917

Li, Y. P., Ding, L., Robinson, A. C., Liu, D. L., Xie, J., Zhang, L. Y., Zhao, C. Y., Yue, Y. H., Liu, Y. D., ... Rajabov, N. (2023). Was cratonic Asia deeply subducted beneath the Pamir? Evidence from P–T conditions and tectonic affinities of Cenozoic Pamir crustal xenoliths. *J. Metamorph. Geol.*, *41*(7), 925–965. https://doi.org/10.1111/jmg.12723

McKenzie, D., Jackson, J., and Priestley, K. (2005). Thermal structure of oceanic and continental lithosphere. *Earth Planet. Sci. Lett.*, *233*(3–4), 337–349. https://doi.org/10.1016/j.epsl.2005.02.005

Mir, R. R., Parvez, I. A., Gaur, V. K., Ashish, Chandra, R., and Romshoo, S. A. (2017). Crustal structure beneath the Kashmir Basin adjoining the western Himalayan syntaxis. *Bull. Seismol. Soc. Am.*, *107*(5), 2443–2458. https://doi.org/10.1785/0120150334

Molnar, P., and Stock, J. M. (2009). Slowing of India's convergence with Eurasia since 20 Ma and its implications for Tibetan mantle dynamics. *Tectonics*, *28*(3), TC3001. https://doi.org/10.1029/2008TC002271

Morley, C. K. (2002). A tectonic model for the Tertiary evolution of strike–slip faults and rift basins in SE Asia. *Tectonophysics*, *347*(4), 189–215. https://doi.org/10.1016/S0040-1951(02)00061-6

Negredo, A. M., Replumaz, A., Villaseñor, A., and Guillot, S. (2007). Modeling the evolution of continental subduction processes in the Pamir–Hindu Kush region. *Earth Planet. Sci. Lett.*, *259*(1–2), 212–225. https://doi.org/10.1016/j.epsl.2007.04.043

Pavlis, G. L., and Das, S. (2000). The Pamir-Hindu Kush seismic zone as a strain marker for flow in the upper mantle. *Tectonics*, *19*(1), 103–115. https://doi.org/10.1029/1999TC900062

Peacock, S. M. (2004). Thermal structure and metamorphic evolution of subducting slabs. In J. Eiler (Ed.), *Inside the Subduction Factory, Volume 138* (pp. 7–22). Washington, DC: American Geophysical Union. https://doi.org/10.1029/138GM02

Peacock, S. M., van Keken, P. E., Holloway, S. D., Hacker, B. R., Abers, G. A., and Fergason, R. L. (2005). Thermal structure of the Costa Rica–Nicaragua subduction zone. *Phys. Earth Planet. Inter.*, *149*(1–2), 187–200. https://doi.org/10.1016/j.pepi.2004.08.030

Qu, R., Zhu, W. L., Ji, Y. F., Xie, C. D., Zeng, D., and Zhang, F. (2023). Subduction thermal regime, petrological metamorphism and seismicity under the Mariana arc. *Sci. Rep.*, *13*(1), 1948. https://doi.org/10.1038/s41598-023-29004-1

Robinson, A. C., Yin, A., Manning, C. E., Harrison, T. M., Zhang, S. H., and Wang, X. F. (2007). Cenozoic evolution of the eastern Pamir: Implications for strain-accommodation mechanisms at the western end of the Himalayan-Tibetan orogen. *GSA Bull.*, *119*(7–8), 882–896. https://doi.org/10.1130/B25981.1

Robinson, A. C., Owen, L. A., Chen, J., Schoenbohm, L. M., Hedrick, K. A., Blisniuk, K., Sharp, W. D., Imrecke, D. B., Li, W. Q., ... Mertz-Kraus, R. (2015). No late Quaternary strike-slip motion along the northern Karakoram fault. *Earth Planet. Sci. Lett.*, *409*, 290–298. https://doi.org/10.1016/j.epsl.2014.11.011

Schmidt, J., Hacker, B. R., Ratschbacher, L., Stübner, K., Stearns, M., Kylander-Clark, A., Cottle, J. M., Alexander, A., Webb, G., ... Minaev, V. (2011). Cenozoic deep crust in the Pamir. *Earth Planet. Sci. Lett.*, *312*(3–4), 411–421. https://doi.org/10.1016/j.epsl.2011.10.034

Schneider, F. M., Yuan, X., Schurr, B., Mechie, J., Sippl, C., Haberland, C., Minaev, V., Oimahmadov, I., Gadoev, M., ... Negmatullaev, S. (2013). Seismic imaging of subducting continental lower crust beneath the Pamir. *Earth Planet. Sci. Lett.*, *375*, 101–112. https://doi.org/10.1016/j.epsl.2013.05.015

Schneider, F. M., Yuan, X., Schurr, B., Mechie, J., Sippl, C., Kufner, S. K., Ratschbacher, L., Tilmann, F., Oimahmadov, I., ... Murodkulov, S. (2019). The crust in the Pamir: Insights from receiver functions. *J. Geophys. Res.: Solid Earth*, *124*(8), 9313–9331. https://doi.org/10.1029/2019JB017765

Schwab, M., Ratschbacher, L., Siebel, W., McWilliams, M., Minaev, V., Lutkov, V., Chen, F. K., Stanek, K., Nelson, B., ... Wooden, J. L. (2004). Assembly of the Pamirs: Age and origin of magmatic belts from the southern Tian Shan to the southern Pamirs and their relation to Tibet. *Tectonics*, *23*(4), TC4002. https://doi.org/10.1029/2003TC001583

Sippl, C., Schurr, B., Tympel, J., Angiboust, S., Mechie, J., Yuan, X., Schneider, F. M., Sobolev, S. V., Ratschbacher, L., ... TIPAGE-Team. (2013a). Deep burial of Asian continental crust beneath the Pamir imaged with local earthquake tomography. *Earth Planet. Sci. Lett.*, *384*, 165–177. https://doi.org/10.1016/j.epsl.2013.10.013

Sippl, C., Schurr, B., Yuan, X., Mechie, J., Schneider, F. M., Gadoev, M., Orunbaev, S., Oimahmadov, I., Haberland, C., ... Radjabov, N. (2013b). Geometry of the Pamir-Hindu Kush intermediate-depth earthquake zone from local seismic data. *J. Geophys. Res.: Solid Earth*, *118*(4), 1438–1457. https://doi.org/10.1002/jgrb.50128

Smith, W. H. F., and Sandwell, D. T. (1997). Global sea floor topography from satellite altimetry and ship depth soundings. *Science*, *277*(5334), 1956–1962. https://doi.org/10.1126/science.277.5334.1956

Sobel, E. R., Schoenbohm, L. M., Chen, J., Thiede, R., Stockli, D. F., Sudo, M., and Strecker, M. R. (2011). Late Miocene–Pliocene deceleration of dextral slip between Pamir and Tarim: Implications for Pamir orogenesis. *Earth Planet. Sci. Lett.*, *304*(3–4), 369–378. https://doi.org/10.1016/j.epsl.2011.02.012

Sobel, E. R., Chen, J., Schoenbohm, L. M., Thiede, R., Stockli, D. F., Sudo, M., and Strecker, M. R. (2013). Oceanic-style subduction controls late Cenozoic deformation of the Northern Pamir orogen. *Earth Planet. Sci. Lett.*, *363*, 204–218. https://doi.org/10.1016/j.epsl.2012.12.009

Stearns, M. A., Hacker, B. R., Ratschbacher, L., Rutte, D., and Kylander-Clark, A. R. C. (2015). Titanite petrochronology of the Pamir gneiss domes: Implications for middle to deep crust exhumation and titanite closure to Pb and Zr diffusion. *Tectonics*, *34*(4), 784–802. https://doi.org/10.1002/2014TC003774

Stübner, K., Ratschbacher, L., Rutte, D., Stanek, K., Minaev, V., Wiesinger, M., and Gloaguen, R. (2013). The giant Shakhdara migmatitic gneiss dome, Pamir, India-Asia collision zone: 1. Geometry and kinematics. *Tectonics*, *32*(4), 948–979. https://doi.org/10.1002/tect.20057

Syracuse, E. M., van Keken, P. E., and Abers, G. A. (2010). The global range of subduction zone thermal models. *Phys. Earth Planet. Inter.*, *183*(1–2), 73–90. https://doi.org/10.1016/j.pepi.2010.02.004

Tackley, P. J., and Xie, S. (2003). STAG3D: A code for modeling thermo-chemical multiphase convection in Earth's mantle. In K. J. Bathe (Ed.), *Computational Fluid and Solid Mechanics 2003* (pp. 1524–1527). Amsterdam: Elsevier. https://doi.org/10.1016/B978-008044046-0.50372-9

Trabant, C., Hutko, A. R., Bahavar, M., Karstens, R., Ahern, T., and Aster, R. (2012). Data products at the IRIS DMC: Stepping stones for research and other applications. *Seismol. Res. Lett.*, *83*(5), 846–854. https://doi.org/10.1785/0220120032

Xu, Q., Zhao, J. M., Yuan, X. H., Liu, H. B., Ju, C. H., Schurr, B., and Bloch, W. (2021). Deep crustal contact between the Pamir and Tarim Basin deduced from receiver functions. *Geophys. Res. Lett.*, *48*(9), e2021GL093271. https://doi.org/10.1029/2021GL093271

Xu, Z. Q., Yang, J. S., Li, H. B., Ji, S. C., Zhang, Z. M., and Liu, Y. (2011). On the tectonics of the India-Asia collision. *Acta Geol. Sin. (in Chinese)*, *85*(1), 1–33. https://doi.org/10.1111/j.1755-6724.2011.00375.x

Yin, A., and Harrison, T. M. (2000). Geologic evolution of the Himalayan-Tibetan orogen. *Annu. Rev. Earth Planet. Sci.*, *28*(1), 211–280. https://doi.org/10.1146/annurev.earth.28.1.211

Yoshii, T. (1975). Regionality of group velocities of Rayleigh waves in the Pacific and thickening of the plate. *Earth Planet. Sci. Lett.*, *25*(3), 305–312. https://doi.org/10.1016/0012-821X(75)90246-0

Zhang, Z. M., Zheng, L. L., Wang, J. L., Zhao, X. D., and Shi, C. (2007). Garnet pyroxenite in the Namjagbarwa Group-complex in the eastern Himalayan tectonic syntaxis, Tibet, China: Evidence for subduction of the Indian continent beneath the Eurasian plate at 80–100 km depth. *Geol. Bull. China (in Chinese)*, *26*(1), 1–12.

Zhao, D. P. (2001). Seismic structure and origin of hotspots and mantle plumes. *Earth Planet. Sci. Lett.*, *192*(3), 251–265. https://doi.org/10.1016/S0012-821X(01)00465-4

Zhong, S. J., Zuber, M. T., Moresi, L., and Gurnis, M. (2000). Role of temperature-dependent viscosity and surface plates in spherical shell models of mantle convection. *J. Geophys. Res.: Solid Earth*, *105*(B5), 11063–11082. https://doi.org/10.1029/2000JB900003

Zhu, W. L., Ji, Y. F., Qu, R., Xie, C. D., and Zeng, D. (2022). Slab metamorphism and interface earthquakes in Peru: Implications from three-dimensional hydrothermal variation in the subducted Nazca plate. *Tectonophysics*, *823*, 229212. https://doi.org/10.1016/j.tecto.2022.229212

Zhu, Y., Ji, Y. F., Zhu, W. L., Qu, R., Xie, C. D., and Zeng, D. (2023). Subduction hydrothermal regime and seismotectonic variation along Kermadec–Tonga megathrusts. *J. Asian Earth Sci.*, *243*, 105532. https://doi.org/10.1016/j.jseaes.2022.105532